

Anti-pausing activity of region 4 of the RNA polymerase σ subunit and its regulation by σ -remodeling factors

Konstantin Brodolin*, Zakia Morichaud

IRIM, CNRS, Univ Montpellier, 1919 route de Mende 34293 Montpellier, France

* corresponding author

Email: konstantin.brodolin@inserm.fr

Keywords: RNA polymerase, abortive transcription, initial pausing, RNA:DNA hybrid, RbpA

ABSTRACT

The basal transcription factors of cellular RNA polymerases (RNAPs) stimulate the initial RNA synthesis via poorly understood mechanisms. Here, we explored the mechanism employed by the bacterial factor σ in promoter-independent initial transcription. We found that the RNAP holoenzyme lacking the promoter-binding domain $\sigma 4$ is ineffective in *de novo* transcription initiation and displays high propensity to pausing upon extension of RNAs 3 to 7 nucleotides in length. The $\sigma 4$ domain stabilizes short RNA:DNA hybrids and suppresses pausing by stimulating RNAP active-center translocation. The anti-pausing activity of $\sigma 4$ is modulated by its interaction with the β subunit flap domain and by the σ remodeling factors AsiA and RbpA. Our results suggest that the presence of $\sigma 4$ within the RNA exit channel compensates for the intrinsic instability of short RNA:DNA hybrids by increasing RNAP processivity, thus favoring productive transcription initiation. This “RNAP boosting” activity of the initiation factor is shaped by the thermodynamics of RNA:DNA interactions and thus, should be relevant for any factor-dependent RNAP.

38 INTRODUCTION

39 Transcription initiation by DNA-dependent RNA polymerase (RNAP) is the first and highly regulated step in
 40 gene expression (Ruff *et al*, 2015)(Saecker *et al*, 2011). After initiation of *de novo* RNA synthesis at
 41 promoters (initial transcription), RNAP fluctuates between promoter escape, which leads to productive RNA
 42 synthesis, and stalling at promoters, which leads to "abortive", reiterative RNA synthesis, a general
 43 phenomenon observed for all RNAPs (Carpousis & Gralla, 1980)(Kubori & Shimamoto, 1996)(Durniak *et*
 44 *al*, 2008) (Murakami *et al*, 2002). Nascent RNA chains longer than 8 nucleotides (nt) form stable, 9- to 10-
 45 base pair (bp)-long RNA:DNA hybrids that are considered a hallmark of the productive elongation complex
 46 (Nudler *et al*, 1997)(Sidorenkov *et al*, 1998)(Kireeva *et al*, 2000) (Kostrewa *et al*, 2009)(Vassylyev *et al*,
 47 2007a). Nascent RNA chains shorter than 9 nt form unstable hybrids with ssDNA templates and tend to
 48 dissociate from the RNAP active site (Metzger *et al*, 1993)(Carpousis & Gralla, 1980)(Sidorenkov *et al*,
 49 1998). However, short RNAs (5-6 nt in length) can be stably bound in the paused initially transcribing
 50 complex (ITC) formed at the *lacUV5* promoter (Brodolin *et al*, 2004)(Duchi *et al*, 2016)(Dulin *et al*, 2018).
 51 The initial transcription pause occurring after the synthesis of 6-nt RNA functions as a checkpoint on the
 52 branched pathway between productive and non-productive transcription (Dulin *et al*, 2018).

53 During RNA synthesis, RNAP performs a stepwise extension of the RNA chain by one nucleotide
 54 that is called nucleotide addition cycle (NAC) (reviewed by (Belogurov & Artsimovitch, 2019). During the
 55 NAC, the first initiating nucleoside triphosphate (NTP) or the 3' end of RNA occupies the product site (i-site)
 56 (pre-translocated state), while the incoming NTP enters in the substrate site (i+1-site). After formation of the
 57 phosphodiester bond, the RNA 3' end moves from the i+1-site to the i-site (post-translocated state). The
 58 concerted translocation of RNA and DNA to the active site is controlled by the β' subunit trigger loop that
 59 folds into the trigger helix upon transition from the pre-translocated to the post-translocated state
 60 (Touloukhonov *et al*, 2007b)(Zhang *et al*, 2010).

61 The basal transcription initiation factors (i.e. bacterial σ subunit, archaeobacterial TFB, and eukaryotic
 62 TFIIB) stimulate the initial steps of RNA synthesis (Kulbachinskiy & Mustaev, 2006)(Werner & Weinzierl,
 63 2005)(Bushnell *et al*, 2004)(Campbell *et al*, 2002)(Zenkin & Severinov, 2004)(Sainsbury *et al*, 2013).
 64 Specifically, the σ subunit region 3.2 hairpin loop (σ 3.2-finger) contacts the template ssDNA strand at
 65 positions -4/-5 and controls its positioning in the active site (Pupov *et al*, 2010)(Tupin *et al*, 2010). The σ 3.2-
 66 finger can indirectly modulate the priming of *de novo* RNA synthesis at promoters (Kulbachinskiy &
 67 Mustaev, 2006)(Pupov *et al*, 2014) and promoter-like DNA templates, such as the M13 phage origin (Zenkin
 68 & Severinov, 2004). The σ subunit may also exert an inhibitory effect on initial transcription. Indeed, the
 69 unstructured linker connecting domains σ 3 and σ 4 (formed by the σ regions 3.2 and 4.1) is located in the
 70 RNA-exit channel and represents a barrier for growing RNA chains. This linker is displaced by RNA upon
 71 promoter escape (Li *et al*, 2020). A clash between the σ 3.2-finger and >4-nt RNA chains hinders RNA
 72 extension and may cause the formation of abortive RNAs, thus contributing to pausing during initial
 73 transcription (Murakami *et al*, 2002)(Basu *et al*, 2014)(Duchi *et al*, 2016)(Zhang *et al*, 2012)(Zuo & Steitz,

74 2015)

75 Binding of the regions σ 3.2 and σ 4.1 within the RNA exit channel takes place during assembly of
76 the RNAP holoenzyme when the σ subunit undergoes the transition from the "closed" to the "open"
77 conformation (Callaci *et al*, 1999). Recent single-molecule fluorescence resonance energy transfer studies
78 demonstrated that in *Mycobacterium tuberculosis*, this transition is regulated by the activator protein RbpA
79 (Vishwakarma *et al*, 2018) that interacts with the σ 2 and σ 3.2 domains (Boyaci *et al*, 2018). Whether RbpA
80 can influence initial transcription has never been explored.

81 Several mechanisms to explain the σ 3.2-finger stimulatory activity during initial transcription have
82 been proposed: (1) stabilization of the template ssDNA in the RNAP active site (Zhang *et al*, 2012); (2)
83 decreased K_m for 3'-initiating NTP binding in the substrate i+1-site (Kulbachinskiy & Mustaev, 2006); and
84 (3) stabilization of short RNAs in the active site (Campbell *et al*, 2002)(Zenkin & Severinov, 2004)(Zenkin
85 *et al*, 2006). The last mechanism was also suggested for the B-reader domain of TFIIB, which is the
86 structural homologue of the σ 3.2-finger (Bushnell *et al*, 2004)(Chen & Hampsey, 2004). As the σ subunit
87 occludes the RNA path and contacts all principal regulatory domains of RNAP (β '-clamp, β -lobe, β -Flap), it
88 may affect RNA synthesis in several ways: through ssDNA template positioning, RNA binding, or direct
89 modulation of the RNAP domain motions.

90 Here, to discriminate among these different scenarios, we investigated how the σ subunit and
91 RNA:DNA hybrid length affect branching between productive and non-productive RNA synthesis during
92 initial transcription by two RNAPs from phylogenetically distant bacterial lineages: *Escherichia coli*
93 (*Eco*RNAP) and *M. tuberculosis* (*Mtb*RNAP). Compared with *Eco*RNAP, *Mtb*RNAP presents several
94 structure-specific features, particularly the lack of *Eco*-specific TL-insertion and the presence of the ~90
95 amino acid-long *Actinobacteria*-specific insertion in the β ' subunit (β '-SI) (Lane & Darst, 2010)(Lin *et al*,
96 2017). To analyze directly the effects of the σ subunit on the RNAP catalytic site activity, we used promoter-
97 less DNA scaffold templates (Tupin *et al*, 2010) (Zenkin & Severinov, 2004). DNA scaffolds have been
98 widely used in structural studies on ITCs of bacterial and eukaryotic RNAPs (Cheung *et al*, 2011) (Liu *et al*,
99 2011). The scaffold model allows bypassing the complexity of promoter-dependent initiation that is strongly
100 influenced by the promoter configuration and by the interactions of σ with promoter elements. When
101 complexed with RNAP, scaffold DNA templates harbor a "relaxed" conformation lacking the topological
102 stress observed in the transcription bubble due to DNA scrunching during initial transcription at promoters.
103 Moreover, as DNA scaffolds lack non-template strand ssDNA, transcription initiation should be less affected
104 by interaction with the core recognition element (CRE) (Vvedenskaya *et al*, 2014). We found that the
105 promoter-binding domain σ 4 (i.e. the structural homologue of the eukaryotic TFIIB B-ribbon), located ~60 Å
106 away from the active site, strongly stimulates RNAP translocation and stabilizes short RNA:DNA hybrids in
107 the RNAP active site. The combination of these activities provides the basis for the initiation-to-elongation
108 transition regulation by the auxiliary transcriptional factors that binds to the σ subunit.

109

110 RESULTS

111 The σ^{70} subunit is required for initial transcription from the promoter-less scaffold DNA template

112 To explore the role of the σ subunit in initial transcription we used two types of minimal DNA scaffold
 113 templates (**Fig. 1A**): a Short Duplex Template (SDT), which included the 9-bp downstream DNA (dwDNA)
 114 duplex, and a Long Duplex Template (LDT), which comprised the 18 bp dwDNA duplex. The dwDNA
 115 duplex of the LDT scaffold forms additional contacts with the β' subunit residues 202-247 that stabilize the
 116 RNAP-scaffold complex (Kulbachinskiy *et al*, 2002)(Vassylyev *et al*, 2007a). Previously, we demonstrated
 117 that extension of the 3-nt RNA primer on SDT DNA is strongly stimulated by the σ^{70} subunit (Tupin *et al*,
 118 2010). Here, we found that the RNAP core from *E. coli* (*Eco*RNAP) was inactive in *de novo* transcription
 119 initiation at SDT and LDT templates performed in the presence of [α - 32 P]-UTP, CTP and GTP (**Fig. 1B**).
 120 Conversely, the σ^{70} -*Eco*RNAP holoenzyme synthesized a single 3-nt RNA (pppC[α - 32 P]UpG) starting 8 nt
 121 downstream of the 3' end of the template DNA (designated as "+1") (**Fig. 1B**). This start site assignment was
 122 validated by using the antibiotic rifampicin that inhibits the synthesis of the second phosphodiester bond.
 123 Indeed, rifampicin addition abolished the formation of 3-nt RNA and induced the accumulation of
 124 radiolabeled 2-nt RNA (pppC[α - 32 P]U) (**Fig. 1C**).
 125

126 The promoter-binding domain $\sigma 4$ is essential for *de novo* initiation of RNA synthesis

127 To identify the σ^{70} regions that influence RNA synthesis initiation on minimal scaffolds, we generated a
 128 panel of σ^{70} mutants (**Fig. 1D, E**). The $\sigma_{\Delta 3-4}$ fragment (residues 1-448) in which the regions 3 and 4 were
 129 deleted, is inactive in promoter-dependent transcription initiation (Zenkin *et al*, 2007). The $\sigma_{\Delta 4}$ fragment
 130 (residues 1-529) lacked part of region 3.2 and the entire $\sigma 4$ domain. In the $\sigma_{\Delta 4.2}$ fragment (residues 1-553),
 131 only region 4.2 was deleted, but not the 4.1 α -helix, which binds inside the RNA exit channel (**Fig. 1E**). In
 132 agreement with previous studies (Kumar *et al*, 1993)(Kumar *et al*, 1994), the *Eco*RNAP holoenzymes
 133 harboring the $\sigma_{\Delta 4}$ or $\sigma_{\Delta 4.2}$ fragments were inactive in abortive transcription assays with the -10/-35 type
 134 *lacUV5* promoter, and displayed reduced transcriptional activity with the "extended -10" type *galP1*cons
 135 promoter (**Fig. 1F**). The $\sigma_{\Delta 3.2}$ subunit, in which residues 513-519 in the $\sigma 3.2$ -finger were deleted, was active
 136 in transcription initiation with both promoters. The *Eco*RNAP holoenzymes assembled with the mutant σ^{70}
 137 subunits were inactive in *de novo* transcription initiation on the SDT scaffold (**Fig. 1B**). We detected no
 138 synthesis of dinucleotide RNA products by the *Eco*RNAP core and by the holoenzyme, differently from what
 139 reported for initial transcription on the M13 minus-strand origin (Zenkin & Severinov, 2004). This difference
 140 might be explained by the low NTP concentration (22 μ M) used in our experiments. Conversely, on the LDT
 141 scaffold, the activity of $\sigma_{\Delta 3.2}$ corresponded to 42% of the activity of full length σ^{70} . Thus, strengthening the
 142 interaction between RNAP and the dwDNA duplex beyond position +10 can compensate for the lack of
 143 interaction between the $\sigma 3.2$ -finger and template-strand ssDNA. This result suggests that the $\sigma 3.2$ -
 144 finger/DNA interaction contributes to, but is not essential for initial transcription. The transcription defects

caused by deletions in domain σ_4 , which does not interact with scaffold DNA, cannot be compensated by the dwDNA interactions, suggesting that $\sigma_{4.2}$ is essential for initial transcription and exerts its activity through interaction with RNAP. Conversely, it has been suggested that σ_4 is dispensable for initial transcription on the M13 phage minus-strand origin (Zenkin & Severinov, 2004). This discrepancy might be caused by differences in the DNA template architecture.

dwDNA duplex and RNA primers suppress the translocation defect caused by deletions in the σ subunit.

In promoter-dependent transcription initiation, short (≤ 3 -nt) RNA primers (pRNAs) can rescue the defects linked to deletions in the $\sigma_{3.2}$ and σ_4 regions (Campbell *et al*, 2002)(Zenkin & Severinov, 2004) (Kulbachinskiy & Mustaev, 2006). To determine whether they have the same effect also when using minimal scaffold templates, we carried out transcription in the presence of a 2-nt pRNA (GpC, pRNA2) the 3' end of which was complementary to the third position upstream of the DNA duplex (designated as position "+1") (**Fig. 2A**). We assumed that the first catalytic step, addition of [α - 32 P]-UTP to pRNA2 (synthesis of GpC[α - 32 P]U), does not require translocation of the RNAP active center because the 3' end of pRNA2 binds to the "product-site" (i-site, facing the position +1 of the DNA template), thus leaving the "substrate site" (i+1, facing position +2 of the DNA template) available for incoming NTP (**Fig. 2B**). This hypothesis is supported by the structures of the RNAP initiation complexes with synthetic scaffolds observed in post-translocated states (Cheung *et al*, 2011)(Zhang *et al*, 2012). The next catalytic steps (synthesis of the GpC[α - 32 P]UpG and GpC[α - 32 P]UpGpA products) require the translocation of the RNA 3' end from the i+1 site to the i-site (**Fig. 2A, B**). As only the first incorporated NTP (U) was labeled, the fraction of the longest reaction product (RNA[N+2]) reflected the overall "efficiency of RNAP translocation" from register +2 to +4.

In the presence of GpC and three nucleotides ([α - 32 P]-UTP, GTP, and ATP), the *Eco*RNAP core synthesized two [32 P]-labeled RNA products (3-nt and 5-nt RNAs), with a bias toward the shorter one (overall translocation efficiency: $\sim 40\%$, **Fig. 2C**). In the same conditions, σ^{70} strongly stimulated [α - 32 P]-UTP incorporation and translocation. Consequently, the 5-nt RNA was the major reaction product synthesized by the *Eco*RNAP holoenzyme (95% translocation efficiency). The observed low efficiency of the [α - 32 P]-UTP-addition reaction by the *Eco*RNAP core might reflect its low affinity for pRNA2. Indeed, increasing pRNA2 concentration increased [α - 32 P]-UTP incorporation, but did not stimulate translocation (**Fig. S1**). Even the "minimal" $\sigma_{\Delta 3-4}$ fragment strongly stimulated [α - 32 P]-UTP incorporation, compared with the *Eco*RNAP core (**Fig. 2D, Fig. S2**). Therefore, binding of domain σ_2 to the *Eco*RNAP core may strengthen its interaction with the scaffold DNA/RNA and/or directs it to the active site cleft.

Like with promoter DNA templates, the initiation defect on DNA scaffolds upon $\sigma_{3.2}$ -finger deletion was rescued by pRNA2 ($\sim 80\%$ translocation efficiency, **Fig. 2C**). The C-terminal deletions in the σ^{70} subunit ($\sigma_{\Delta 3-4}$, $\sigma_{\Delta 4}$ and $\sigma_{\Delta 4.2}$) hindered the synthesis of 5-nt RNA ($<50\%$ translocation efficiency) leading to RNA

patterns similar to those of the *Eco*RNAP core. As deletion of the region 4.2 and deletion of the entire $\sigma 3$ and $\sigma 4$ domains led to the same effect, we conclude that $\sigma 4.2$ is a principal determinant for the efficient synthesis of the 5-nt RNA product. It is unlikely that the translocation defect conferred by deletion of the region $\sigma 4.2$ is due to a decreased affinity of the 3-nt RNA product (GpC[α - 32 P]U) for the RNAP active site because the overall [α - 32 P]-UTP incorporation was similar with full length σ^{70} and $\sigma_{\Delta 4.2}$ (**Fig. 2C**). Our results suggest that RNAP translocation from register +2 to register +3 is a rate-limiting step for 5-nt RNA synthesis, and is slower than [α - 32 P]-UTP addition and the 3-nt RNA product dissociation. The $\sigma 4$ deletions had similar effects on translocation also when using the SDT scaffold and the 3-nt pRNA (CpGpC, pRNA3) (**Fig. S2**). However, the 3-nt pRNA suppressed the transcription defects caused by the $\sigma 4$ deletion on the LDT but not the SDT scaffold, indicating the RNAP interaction with dwDNA stimulates translocation. To explore the effect of the DNA duplex on RNAP translocation we used modified versions of the SDT scaffold (SDT2 and SDT2+1), with more stable dwDNA duplexes (**Fig. 2D**). Moreover, in the SDT2+1 scaffold, the 5' end upstream edge of the DNA duplex was extended by one base pair (G:C). Thus, translocation from register +2 to register +3 on SDT2+1 requires the unpairing of 1 bp of dwDNA followed by the formation of the contact between G at position +3 of the non-template DNA and the CRE pocket of the RNAP core that is known to counteract transcriptional pausing (Vvedenskaya *et al*, 2014). Translocation was more efficient on the SDT2+1 scaffold compared with the SDT1 scaffold (**Fig. 2E**), suggesting that dwDNA duplex melting is not a barrier for translocation and that the interaction with CRE stimulates translocation. We conclude that *Eco*RNAP pauses after the addition of the first NTP to the RNA primer and that the interaction with the downstream DNA and RNA promotes forward translocation. The region $\sigma 4.2$ may act on translocation by strengthening this interaction.

The σ subunit regions 3.2 and 4.2 stabilize ≤ 4 -nt RNAs in the RNAP active site

To determine whether the σ subunit can stabilize short RNAs in the RNAP active site, we immobilized ITCs on Ni²⁺-agarose beads and tested their ability to retain RNAs by washing the complexes with transcription buffer. We used 2 to 6 nt-long pRNAs the 3' end of which was aligned to the same position of the template, designated as position "+1" (**Fig. 3A**) Control experiments in which complexes were formed by the core *Eco*RNAP on SDT and LDT scaffolds showed that after washing with the "high salt" buffer containing 1M NaCl (**Fig. S3**), 5-, 6-, 7-, 13-nt pRNAs were stably bound in ITCs. However, reduced retention of 5- and 6-nt pRNAs, was observed with the SDT scaffold. This indicates that the dwDNA duplex contributes to the overall stabilization of the complex. Consequently, the LDT scaffold was used in the next experiments. To measure the retention efficiency, ITCs containing 2- to 6-nt RNAs were either washed with the transcription buffer containing 250 mM NaCl and then labeled with [α - 32 P]-UTP, or directly labeled without washing step (**Fig. 3B**). This experiment demonstrated that 2- to 4-nt pRNAs were weakly bound to ITCs compared with 5- to 6-nt pRNAs (**Fig. 3B-D**). Therefore, the 4-bp RNA:DNA hybrid is a conversion point between stable and unstable ITC states. Moreover, we observed a clear difference in the capacity to hold 4-nt pRNA by ITCs

containing the full length σ subunit (75% retention efficiency) and σ mutants ($\sigma_{\Delta 3.2}$ and $\sigma_{\Delta 4}$; <50% retention efficiency) (**Fig. 4E**). The defect was stronger for $\sigma_{\Delta 4}$ -*Eco*RNAP than $\sigma_{\Delta 3.2}$ -*Eco*RNAP. We obtained similar result with the SDT scaffold (**Fig. S4**). To determine whether the slight difference in 4-nt pRNA retention observed between $\sigma_{\Delta 3.2}$ and $\sigma_{\Delta 4}$ (**Fig. 4E**) was significant, we performed several washing steps on ITCs formed by $\sigma_{\Delta 3.2}$ -*Eco*RNAP and $\sigma_{\Delta 4.2}$ -*Eco*RNAP (**Fig. 4F,G**). After the third washing step, almost no bound RNA was left in $\sigma_{\Delta 4.2}$ -ITC (~10% retention relative to full length σ^{70}), while RNA retention was higher for $\sigma_{\Delta 3.2}$ -ITC (~40% retention relative to full length σ^{70}). RNA binding remained stable with wild type σ^{70} -ITC (60% retention relative to the 'no washing' condition). We conclude that the σ^{70} subunit stabilizes 4-5-nt-long RNAs in the RNAP active site and that the region $\sigma 4.2$ is a major determinant of this activity.

226

227 The σ region 4.2 promotes extension of ≤ 7 nt-long RNAs

To explore the relationship between translocation efficiency and RNA:DNA hybrid stability, we performed 2-min primer extension reactions with pRNAs of various lengths in the presence of [α - 32 P]-UTP, GTP and ATP (**Fig. 4A**). In these experiments, to facilitate the detection of the initial pause, we used the SDT scaffold that displayed stronger σ -dependence in translocation. The *Eco*RNAP core efficiently extended ≥ 8 -nt pRNAs (>90% efficiency) (**Fig. 4B,C**), and its translocation efficiency decreased gradually with the RNA length shortening. This dependence on RNA length might be explained by the intrinsic instability of RNA:DNA hybrids and/or by the disengagement of the RNA 3' end from the active site. The translocation efficiency was independent from the RNA length when the wild type *Eco*RNAP holoenzyme was used (**Fig. 4B,C**). The $\sigma_{\Delta 3.2}$ -*Eco*RNAP holoenzyme displayed strong translocation defects with 3-nt pRNA (~25% efficiency), moderate defects with 4-5-nt pRNAs (~80% efficiency), and no defect with 6-nt pRNA (>90% efficiency). On the basis of the RNAP-promoter complex structure data, the 5' end of ≥ 5 -nt-long RNAs clashes with the $\sigma 3.2$ -finger (**Fig. 4D**). Thus, the $\sigma 3.2$ -finger should hinder the extension of RNAs longer than 5 nt and favor abortive initiation (Murakami *et al*, 2002)(Li *et al*, 2020). A model of the $\sigma 3.2$ -finger deletion on the *Eco*RNAP structure (**Fig. 4E**) showed that 5-to 7-nt RNAs can be accommodated in the active site cleft. Yet, the remaining segment of the region $\sigma 3.2$ can still contact the template DNA strand at positions -6/-7. Strikingly, in our experiments, 'abortive' RNAs accumulated when using the *Eco*RNAP core and the $\sigma_{\Delta 3.2}$ -*Eco*RNAP holoenzyme, but not with the wild type *Eco*RNAP holoenzyme. This suggests that the $\sigma 3.2$ -finger is not the primary cause of abortive RNA formation and that abortive RNA synthesis is not an obligatory event in initiation (Duchi *et al*. 2016).

Unlike $\sigma_{\Delta 3.2}$ -*Eco*RNAP, translocation stimulation was defective with the $\sigma_{\Delta 4.2}$ -*Eco*RNAP holoenzyme and pRNAs shorter than 8 nt. The properties of the $\sigma_{\Delta 4.2}$ -*Eco*RNAP holoenzyme were identical to those of the *Eco*RNAP core except with 5-nt-long RNA that displayed increased translocation efficiency with the *Eco*RNAP core. We did not investigate the reason of this unusual behavior. The results of the "RNA-retention" experiments in combination with the "translocation-dependence" experiments demonstrated that

there is no correlation between RNA:DNA hybrid stability and translocation efficiency. Indeed, 5- and 6-nt RNAs were stably bound to ITC, but still displayed σ -dependence for translocation. Thus, we conclude that the low efficiency in nascent RNA extension (any lengths) by the $\sigma_{\Delta 4.2}$ -*Eco*RNAP holoenzyme is due to RNAP pausing after the first NTP addition, and that the stimulation of RNAP translocation by σ is unlikely to occur through RNA:DNA hybrid stabilization.

The RNA 3' end nucleotide identity determines the initial-transcription pause duration

To explore the impact of $\sigma_{4.2}$ on pausing, we studied the kinetics of 5-nt and 7-nt RNA synthesis initiated with pRNA3 (ITC3, unstable RNA:DNA hybrids) and pRNA5 (ITC5, stable RNA:DNA hybrids), respectively (**Fig. 5A**). The overall $[\alpha\text{-}^{32}\text{P}]\text{-UTP}$ addition rate was similar for ITC3 and ITC5 in the presence of the $\sigma_{\Delta 4.2}$, and was highest in the presence of the full length σ^{70} (**Fig. 5B,C**). Translocation from register +4 to +5 was at least 100-fold faster ($t_{1/2} \sim 1.7$ s) in the presence of full length σ^{70} than of the $\sigma_{\Delta 4.2}$ mutant ($t_{1/2} \sim 200$ s) (**Fig. 5B,D**). Reactions were completed in 120 s, without any further incorporation of $[\alpha\text{-}^{32}\text{P}]\text{-UTP}$. Therefore, the labeled 5-nt RNA product remained bound to RNAP. Extension of the pRNA 5' end by 2 nucleotides (**pRNA5**) accelerated the forward translocation only by 2-fold. Therefore, in agreement with the conclusion drawn in the previous section, the overall RNA:DNA hybrid stabilization has little effect on pausing.

In our assay, the RNA chain elongation starts with addition of U that forms an unstable U:dA pair with the DNA template (Huang *et al*, 2009). Therefore, the 3' end nucleotide might disengage from the active site, and induce pausing. If this hypothesis is correct, the substitution of the U:dA pair by the more stable C:dG pair should suppress pausing, and favor forward translocation. To test this assumption, we used a scaffold (SDT-G) harboring G instead of A at position +2 (**Fig. 5A**), and initiated the primer extension with $[\alpha\text{-}^{32}\text{P}]\text{-CTP}$. Unlike UTP, the CTP addition rate with the $\sigma_{\Delta 4.2}$ -*Eco*RNAP holoenzyme was close to that observed with the wild type *Eco*RNAP holoenzyme (compare **Fig. 5C and 5F**). Thus, without σ_4 , *Eco*RNAP senses the difference between UTP and CTP, while CTP suppresses the effect of the σ_4 deletion. Irrespectively of the RNA length (4-nt or 6-nt), translocation of the mutant $\sigma_{\Delta 4.2}$ -*Eco*RNAP from the register +2 to the register +3 was accelerated by ~ 10 -fold on SDT-G DNA compared with SDT-A DNA. This suggests that the stability of base pairing at the 3' end, but not the RNA:DNA hybrid length is crucial for forward translocation. As $\sigma_{\Delta 4.2}$ -*Eco*RNAP translocation rate was significantly reduced even when the RNA 3' end was stabilized, compared with wild type *Eco*RNAP, we conclude that the region $\sigma_{4.2}$ may affect the active site cycling or the clamp opening-closing dynamics that control RNAP translocation.

The σ_4 remodeling co-activator AsiA stimulates pausing

Region $\sigma_{4.2}$ binds to the flap-tip-helix (FTH) of the RNAP β subunit (Kuznedelov *et al*, 2002) (Geszvain *et al*, 2004) that is implicated in the regulation of pausing (Kang *et al*, 2018). To test whether $\sigma_{4.2}$ exerts its effect on RNA synthesis through interaction with β -FTH, we used the T4 phage co-activator protein AsiA.

288 AsiA remodels exactly the same region in the σ^{70} subunit (residues 528 - 613) that was deleted in the $\sigma_{\Delta 4}$
 289 mutant, and disrupts the interaction between $\sigma 4.2$ and β -FTH (Hinton & Vuthoori, 2000) (Shi *et al*, 2019)
 290 (model in **Fig. 6A**). If the $\sigma 4.2$ - β -FTH contact were essential for RNA synthesis, AsiA should fully inhibit
 291 initial transcription. To test this hypothesis, we performed *de novo* and primed transcription by the σ^{70} -
 292 *Eco*RNAP and $\sigma_{\Delta 4.2}$ -*Eco*RNAP holoenzymes, with and without AsiA, on the SDT2 template (**Fig. 6B**). As
 293 control, we used an abortive transcription assay on the *lacUV5* promoter. AsiA inhibited *lacUV5*-dependent
 294 transcription initiation by 85% (**Fig. 6B, lanes 1,2 and Fig. 6C**). Conversely, *de novo* initiation from the
 295 scaffold was much less sensitive to AsiA. Indeed, 3-nt RNA synthesis was inhibited only by 50%, which
 296 coincided with the accumulation of the short 2-nt RNA product (**Fig. 6B, lanes 7,8 and Fig. 6C**). AsiA also
 297 influenced transcription initiated with the GpC primer (**Fig. 6B, lanes 3,4 and Fig. 6C**). The amount of 3-nt
 298 RNA increased simultaneously with the increase in total [α - 32 P]-UTP incorporation. Such effect was
 299 consistent with the AsiA-induced destabilization of short RNAs, leading to accumulation of “abortive”
 300 transcripts. The finding that AsiA did not affect [α - 32 P]-UTP incorporation with the $\sigma_{\Delta 4}$ -*Eco*RNAP
 301 holoenzyme (**Fig. 6B, lanes 5,6 and Fig. 6C**) indicates that AsiA modulates RNA synthesis through $\sigma 4$.
 302 However, the weak impact of AsiA on initial transcription was in striking contrast with the strong inhibitory
 303 effect of the $\sigma 4$ deletion. The only possible explanation for this discrepancy can be that the $\sigma 4$ physical
 304 presence in the RNA exit channel is essential for initial transcription. In the presence of AsiA, the $\sigma 4$ domain
 305 remains bound inside the RNA exit channel (Shi *et al*, 2019), and therefore AsiA exerts only a weak effect on
 306 scaffold-dependent transcription. We conclude that the interaction of $\sigma 4.2$ with β -FTH modulates the
 307 catalytic site activity, but is not essential for initial transcription.

308 309 **RbpA from *M. tuberculosis* stimulates translocation through the $\sigma 4.2$ / β -FTH interaction**

310 To determine whether the σ subunit anti-pausing activity can be observed with RNAP from other bacteria,
 311 we studied initial transcription by *Mtb*RNAP. We used the *M. tuberculosis* σ^B subunit that requires the
 312 activator protein RbpA to stabilize its active conformation in the *Mtb*RNAP holoenzyme (Vishwakarma *et al*,
 313 2018). As RbpA N-terminus binds within the RNA-exit channel, it could modulate $\sigma 4.2$ anti-pausing activity
 314 (model in **Fig. 6D**). First, we compared the kinetics of 5-nt pRNA extension by *Mtb*RNAP and *Eco*RNAP on
 315 SDT2 DNA in the presence of [α - 32 P]-UTP and GTP (**Figure S5**). As observed with *Eco*RNAP, *Mtb*RNAP
 316 paused at the register +6 during initiation from pRNA5, and its translocation was stimulated by the σ^B -RbpA
 317 complex. To better understand the role of $\sigma 4.2$ - β -FTH interaction in initial pausing, we constructed a
 318 *Mtb*RNAP mutant in which the β subunit residues 811-825 were deleted (*Mtb*RNAP $^{\Delta FTH}$), and then assessed
 319 how the translocation activity of the mutant and wild type enzymes were influenced by the pRNA length
 320 (**Fig. 6E,F**). ITCs were assembled with 2, 3, 5 and 6-nt pRNAs (ITC2 to 6) in the presence of σ^B and RbpA,
 321 or without transcription factors, and supplemented with [α - 32 P]-UTP and GTP. As observed with *Eco*RNAP,
 322 *Mtb*RNAP translocation efficiency increased gradually with the RNA length, and reached 80% with the 6-nt

323 pRNA. Like for σ^{70} , the σ^B -RbpA complex stimulated the forward translocation with short pRNAs (3-6-nt in
324 length). However, the σ^B subunit alone did not stimulate translocation, in agreement with fact that its
325 conformation in the *Mtb*RNAP holoenzyme differs from that of σ^{70} in the *Eco*RNAP holoenzyme. The
326 deletion of β -FTH abolished σ^B anti-pausing activity with ITC2 and ITC3 (2- and 3-nt pRNAs, respectively).
327 Furthermore, the RNA amount produced by unstable ITC2/ ITC3 formed by the *Mtb*RNAP^{ΔFTH} mutant
328 increased by ~4-fold, compared with the amount produced by the stable ITC6. (**Fig. S6**). This “abortive-like”
329 behavior was observed only in the presence of the σ^B subunit, and might be caused by a clash between the
330 inappropriately positioned region 3.2 and RNA. Addition of RbpA only partially restored σ^B capacity to
331 stimulate *Mtb*RNAP^{ΔFTH} translocation (**Fig. 6F and Fig. S5**). In agreement with the conclusion drawn from
332 the experiments with AsiA, this result suggests that $\sigma^{4.2}$ interaction with β -FTH regulates, but is not
333 essential for the anti-pausing activity of σ^B . The β -FTH deletion should dramatically destabilize σ^4
334 positioning/interaction within RNA channel and consequently enhance pausing and abortive transcription.
335 RbpA compensates for the lack of β -FTH probably by facilitating σ^4 positioning within the RNA-exit
336 channel.

337

338 DISCUSSION

339 Our study demonstrates that RNAPs from different bacterial species, are inefficient in initial transcription
340 and prone to pause upon extension of short RNAs (3 to 7-nt in length). The σ subunit region 4.2, which was
341 implicated only in promoter binding, counteracts the initial transcription pausing and thus plays an essential
342 role in organizing of the RNAP active center for efficient initiation of *de novo* RNA synthesis. The $\sigma^{4.2}$
343 region displays two distinct activities: RNA:DNA hybrid-stabilizing activity, and translocation-stimulating
344 activity. Modulation of these activities by the σ -remodeling factors may be a general mechanism to tune
345 initial transcription.

346

347 Initial transcription pausing on the pathway to abortive transcription

348 Our results suggest that at each nucleotide addition step, ITCs harboring 3-8 nt RNAs can enter into a paused
349 state in which the RNA 3' end is disengaged from the active site. The paused ITC (PITC) bifurcates in two
350 pathways: abortive pathway in which nascent RNA dissociates from RNAP, and productive pathway in
351 which nascent RNA remains bound to RNAP and slowly translocates to the next register (**Figure 7**). PITC
352 conversion to productive ITC is accelerated by (1) strengthening the dwDNA/RNAP interactions, (2)
353 strengthening the RNA:DNA hybrid /RNAP interactions, and (3) stabilizing base pairing at the RNA 3' end.
354 These observations can be explained by a simple model in which the lack of the stable 9-bp RNA:DNA
355 hybrid impedes the concerted translocation of RNA and DNA. During NAC, the RNAP pincers formed by
356 the β' clamp and β lobe should transiently adopt an open or partially open conformation (Vassylyev *et al*,
357 2007b)(Weixlbaumer *et al*, 2013). We speculate that this opening may weaken the RNAP interaction to hold
358 together template DNA and RNA. Due to the thermal motions and the altered, misaligned structure of short

RNA:DNA hybrids (Liu *et al*, 2011) (Cheung *et al*, 2011), the RNA 3' end may be displaced from the active site. In addition, the 3'-U forms unstable base pairs (U:dA) that in the absence of $\sigma 4$, may favor the formation of the frayed state, leading to backtracking and pausing (Artsimovitch & Landick, 2000) (Touloukhonov *et al*, 2007a). Consequently, the PITC remains blocked in one of the inactive states (half-translocated, hyper-translocated, or backtracked) that slowly isomerize to an active post-translocated state. The 3'-C that forms more stable (C:dG) base pairs remains in the active site, thus promoting forward translocation. In support to this model, the PITC half-life time was more strongly biased by the RNA 3' end nucleotide identity than by the RNA:DNA hybrid length. Indeed, the RNA 3' end nucleotide also modulated the translocation bias in stable elongation complexes with 8- 9-bp RNA:DNA hybrids (Hein *et. al*, 2011). The σ subunit may restrain RNA and DNA motions by strengthening the RNAP core interactions with RNA and DNA, thus allowing the correct alignment of the template to the active site and promoting translocation. The σ -mediated stabilization of short RNAs in the active site and stimulation of the forward translocation should drastically reduce the probability of abortive transcription and shift the equilibrium toward promoter escape. As the half-life time of the initial pause strongly depends on the RNA 3' end nucleotide identity, it should be a promoter-specific event determined by the initial transcribing DNA sequence.

Two steps in the maturation of RNA:DNA hybrids and DNA scrunching

Our results underline two phases in initial transcription: (1) transition from unstable to stable RNA:DNA hybrids when RNA length reaches 5 nt; and (2) transition from ITC prone to pause to productive ITC/EC when RNA length exceeds 8 nt (**Figure 7B**). Before the first phase, abortive transcription is predominant and the RNA:DNA hybrid stability depends on σ . Before the second phase, pausing is predominant and translocation depends on σ . These phases perfectly fit with the three ITC types observed at natural promoter templates: unstable ITCs with RNAs < 4 nt, intermediate stability ITCs with RNAs of 4-8 nt, and stable productive ITC with RNAs > 8 nt (Metzger *et al*, 1993)(Carpousis & Gralla, 1980). Our results on RNA:DNA hybrid stability are in agreement with structural studies on eukaryotic RNAPII showing that ITCs with 4-5-nt RNAs form distorted or mismatched RNA:DNA hybrids, while the 6-8 bp hybrids harbor identical canonical structures (Liu *et al*, 2011). Unlike ITCs formed on promoters, ITCs formed on our DNA scaffolds lack the upstream part of the transcription bubble and non-template ssDNA. Therefore, the initial transcription on scaffold is not affected by the stress arising due to DNA scrunching, which is a major cause of abortive transcription (Kapanidis *et al*, 2006). The lack of stress in DNA templates may explain the quantitative retention of 4-7-nt RNAs in σ -containing ITCs formed on scaffolds, compared with the a small fraction of 5 to 7-nt RNAs retained in ITCs formed on promoter DNA templates (Brodolin *et al*, 2004)(Duchi *et al*, 2016).

$\sigma 4$ versus $\sigma 3.2$ -finger

We found that the region 4.2 of the σ subunit stimulates *de novo* initiation, stabilizes short RNA:DNA

hybrids, and selectively stimulates UTP addition to the RNA 3' end. These activities were previously attributed to the σ 3.2-finger (Kulbachinskiy & Mustaev, 2006)(Pupov et al, 2014)(Zenkin & Severinov, 2004) that stabilizes template ssDNA in the active site (Zhang et al, 2012)(Tupin et al, 2010). Altogether, our results show that σ 4.2 activity during initial transcription can be clearly differentiated from that of the σ 3.2-finger. Indeed, σ 3.2-finger deletion abolished RNA retention in ITCs, but had only a moderate effect on translocation. Conversely, σ 4 deletion strongly affected RNA retention and also translocation. Furthermore, the σ 3.2-finger was dispensable for *de novo* initiation on scaffold template harboring a long dwDNA duplex, while σ 4.2 was essential. Therefore, we conclude that σ 4 interaction with core RNAP is a major determinant of the σ subunit transcription-stimulatory activities. Our results also suggest that the σ 3.2 and σ 4 regions are functionally connected, and changes in σ 3.2 structure may affect σ 4 function. Therefore, the σ 3.2-finger deletion might have an impact on promoter-dependent transcription via allosteric changes in σ 4 conformation or/and its positioning in the RNA exit channel. Finally, our results provide a rational explanation to the finding that defects caused by σ 3.2-finger deletion are promoter-sequence dependent (Kulbachinskiy & Mustaev, 2006)(Morichaud *et al*, 2016).

The σ subunit domain 4 as allosteric regulator of NAC

The domain σ 4 does not make any contact with the scaffold DNA or RNA, and therefore exerts its anti-pausing activity through interaction with the RNAP core. In the RNAP holoenzyme, the region 4.1 of σ 4 is located in the RNA exit channel and occupies the place of RNA, 13-16 nucleotides from the RNA 3' end. Region 4.2 of σ 4 interacts with β -FTTH. Therefore, σ 4 may influence translocation, like the RNA structures formed within the RNA-exit channel that can affect RNAP active site conformational cycling (trigger loop folding/unfolding) through β -flap interaction (Touloukhonov & Landick, 2003)(Touloukhonov *et al*, 2001) (Hein *et al*, 2014). In addition, σ 4.2 interaction with the Zn-binding domain of the β' -clamp might influence clamp conformational motions during translocation. Paused elongation complexes are characterized by several changes in RNAP structure: rotation of the swivel module (comprising the β' clamp), disordered β -flap (Kang *et al*, 2018), widened RNA exit channel, and partially open clamp state (Weixlbaumer *et al*, 2013). The PITC complexes formed in our assay likely resemble the crystallized elemental paused elongation complexes (ePEC) formed with scaffolds the architecture of which was almost identical to ours (lacking non-template strand ssDNA) and that were trapped in a partially open clamp conformation (Weixlbaumer *et al*, 2013). We hypothesize that in the absence of 9-bp RNA:DNA hybrids and σ 4, RNAP may be blocked in the open-clamp/non-swiveled state, thus inhibiting forward translocation. The σ 4 interaction with the RNA exit channel/clamp may promote conformational motions of the swivel module/clamp and thus stimulate translocation during initial transcription.

Analogy in function of the basal transcription factors from different kingdoms of life

We demonstrated that the anti-pausing activity can be observed with structurally distinct σ subunits and phylogenetically distant RNAPs (*E. coli* and *M. tuberculosis*). Considering that the $\sigma 4$ and β -flap interaction is invariant between all classes of σ subunits, we propose that σ anti-pausing activity is an universal feature of initial transcription in bacteria. We hypothesize that the function mechanism of archaeal TFB and eukaryotic TFIIB, which are implicated in RNA synthesis priming, might be similar to that of the σ subunit. Indeed, TFIIB, in which B-reader and B-ribbon are topological homologues of $\sigma 3.2$ and $\sigma 4$ respectively (Liu *et al*, 2010)(Kostreva *et al*, 2009), can stabilize 5-nt RNA in ITC (Bushnell *et al*, 2004) and stimulate *de novo* transcription initiation on scaffold templates (Sainsbury *et al*, 2013).

MATERIALS AND METHODS

Proteins, DNA templates, and RNA oligonucleotides

Recombinant core RNAP (harboring the C-terminal 6xHis-tag on rpoC) of *E. coli* (expression plasmid pVS10) and *M. tuberculosis* (expression plasmid pMR4) were expressed in *E. coli* BL21(DE3) cells and purified as described before (Hu *et al*, 2014) (Morichaud *et al*, 2016). The σ^{70} and σ^B subunits and their mutants (harboring an N-terminal 6xHis-tag) were constructed and produced as described (Hu *et al*, 2014) (Morichaud *et al*, 2016)(Zenkin *et al*, 2007). RNA oligonucleotides were purchased from Eurogentec and DNA oligonucleotides from Sigma-Aldrich. All oligonucleotides were HPLC purified. AsiA was a generous gift from Dr. Deborah Hinton. The 116bp *lacUV5* was prepared by PCR amplification (Morichaud *et al*, 2016). The 72-bp *galP1*cons promoter fragment (promoter positions -50 to +22) was prepared by annealing two oligonucleotides (upper strand oligonucleotide labeled by Cy3 at the 5' end: 5'-GTTTATTCCA TGTCACACTT TTCGCATCTT TTCGTTGCTA TAATTATTTC ATACCAAAG CCTAATGGAG CG-3', and bottom strand: 5'-CGCTCCATTA GGCTTTTGGT ATGAAATAAT TATAGCAACG AAAAGATGCG AAAAGTGTGA CATGGAATAA AC-3') followed by purification on 10% PAGE. To assemble DNA scaffolds, oligonucleotides were heated in transcription buffer (TB; 40 mM HEPES pH 7.9, 5mM MgCl₂ 50 mM NaCl, 5% glycerol) at 65°C for 5 min, and then annealed by lowering the temperature to 16°C for 30 min.

Scaffold-based transcription assays

Transcription reactions were performed in 5 μ l of TB. 240 nM RNAP core was mixed with 1 μ M of full length σ or 2 μ M of σ mutants, and incubated at 37°C for 5 min. 1 μ M RbpA was added when indicated. Samples were supplemented with 0.8 μ M (final concentration) scaffold DNA and 50 μ M (final concentration) pRNA. The primer extension kinetics were evaluated using 100 μ M pRNA. Samples were incubated on ice for 5 min, then at 22°C for 5 min, and supplemented with 0.4 μ M [α -³²P]-UTP or [α -³²P]-CTP and 22 μ M of the indicated NTPs (HPLC purified). Transcription was performed at 22°C for 2 min or for the indicated time and stopped by adding an amount of loading buffer (8M Urea, 50mM EDTA, 0.05% bromophenol blue) equal to the reaction volume. Samples were heated at 65°C for 2 min and RNA products

were resolved on 26% PAGE (acrylamide : bis-acrylamide ratio 10:1) with 7M urea and 1x TBE.

RNA retention assay

*Eco*RNAP-scaffold DNA-RNA complexes were assembled as described above except that 100 μ M of 2-3-nt pRNA and 10 μ M of 4-5-nt pRNA were used. pRNA7 and pRNA13 were mixed with scaffold DNA before annealing. Complexes formed in 5 μ l TB in Axygen® 1.7 ml MaxyClear Microtubes were incubated at 18°C for 5 min. Then, 5 μ l of Ni-NTA agarose beads slurry (Qiagen) in TB was added, and tubes shaken using an Eppendorf ThermoMixer® at 18°C for 5 min. To separate the Ni-bound RNAP fraction, 0.5 ml of TB/250mM NaCl was added. Samples were briefly stirred, pelleted by centrifugation at 1000g for 1 min, and supernatants were discarded. A second washing step was performed with 50 μ l of TB as before. Supernatants were removed to leave a sample volume of 10 μ l. [α -³²P]-UTP (0.4 μ M final concentration) was added to all samples that were then incubated at 22°C for 3 min. Reactions were quenched and analyzed as above.

Promoter-based transcription assays

Transcription on the *lacUV5* and *galP1cons* promoters was performed with 200 nM *Eco*RNAP, 500 nM full length σ^{70} or 2 μ M σ^{70} mutants, and 300 nM DNA template in TB. Samples were incubation at 37° for 10 min, and supplemented with 100 μ M ApA (*lacUV5* assay) or CpA (*galP1cons* assay) and 0.4 μ M [α -³²P]-UTP. Transcription reactions were performed at 37°C for 10 min.

AsiA inhibition assay

500 nM σ^{70} was first mixed with 1 μ M AsiA and then with 100 nM *Eco*RNAP core. Samples were incubated at 30°C for 10 min. Next, DNA templates were added and samples were incubated at 30°C (with *lacUV5* promoter) and at 22°C (with SDT2 scaffold) for 5 min. Transcription from the *lacUV5* promoter (50 nM) was initiated by adding 100 μ M ApA and 0.4 μ M [α -³²P]-UTP at 37°C for 5 min. Transcription from scaffold DNA (0.8 μ M) was performed in the presence of 0.4 μ M [α -³²P]-UTP and 25 μ M NTPs or 50 μ M GpC and carried out at 22°C for 3 min.

Calculation of the pause half-life times

The pause half-life times ($t_{1/2} = \ln 2/k$) were calculated by fitting the fractions of RNA in pause $[P_i^{PS}]/[P_i^{total}]$ in function of the time t using the following single-exponential equation: $[P_i^{PS}]/[P_i^{total}] = A_0 \cdot \exp(-k \cdot t) + R$, where $[P_i^{PS}]$ is the RNA in pause at the time point i and $[P_i^{total}]$ is the total RNA at the time point i . A_0 is the amplitude and R is the residual.

ACKNOWLEDGMENTS

We thank Georgiy Belogurov for discussion of the results and Nikolay Zenkin for critical reading. We are grateful to Deborah Hinton for providing AsiA protein. Funding was from the French National Research

502 Agency [MycoMaster ANR-16-CE11-0025-01].

503

504 **AUTHOR CONTRIBUTIONS**

505 K.B conceived the study and designed experiments, K.B. and Z.M. performed experiments. K.B. performed
506 data analysis and wrote the manuscript with contribution from Z.M.

507

508 **CONFLICT OF INTEREST**

509 The authors declare that they have no conflict of interest.

513 **REFERENCES**

- Artsimovitch I & Landick R (2000) Pausing by bacterial RNA polymerase is mediated by mechanistically distinct classes of signals. *Proc. Natl. Acad. Sci. U. S. A.* **97**: 7090–7095
- Basu RS, Warner B a, Molodtsov V, Pupov D, Esyunina D, Fernandez-Tornero C, Kulbachinskiy A & Murakami KS (2014) Structural Basis of Transcription Initiation by Bacterial RNA Polymerase holoenzyme. *J. Biol. Chem.*: M114.584037–
- Belogurov GA & Artsimovitch I (2019) The Mechanisms of Substrate Selection, Catalysis, and Translocation by the Elongating RNA Polymerase. *J. Mol. Biol.* **431**: 3975–4006
- Boyaci H, Chen J, Lilic M, Palka M, Mooney RA, Landick R, Darst SA & Campbell EA (2018) Fidaxomicin jams Mycobacterium tuberculosis RNA polymerase motions needed for initiation via RbpA contacts. *eLife* **7**: Available at: <https://elifesciences.org/articles/34823>
- Brodolin K, Zenkin N, Mustaev A, Mamaeva D & Heumann H (2004) The sigma 70 subunit of RNA polymerase induces lacUV5 promoter-proximal pausing of transcription. *Nat Struct Mol Biol* **11**: 551–7
- Bushnell D a, Westover KD, Davis RE & Kornberg RD (2004) Structural basis of transcription: an RNA polymerase II-TFIIB cocrystal at 4.5 Angstroms. *Science* **303**: 983–988
- Callaci S, Heyduk E & Heyduk T (1999) Core RNA polymerase from E. coli induces a major change in the domain arrangement of the sigma 70 subunit. *Mol Cell* **3**: 229–38
- Campbell E a, Muzzin O, Chlenov M, Sun JL, Olson CA, Weinman O, Trester-Zedlitz ML & Darst S a (2002) Structure of the bacterial RNA polymerase promoter specificity sigma subunit. *Mol. Cell* **9**: 527–539

- Carpousis AJ & Gralla JD (1980) Cycling of ribonucleic acid polymerase to produce oligonucleotides during initiation in vitro at the lac UV5 promoter. *Biochemistry* **19**: 3245–3253
- Chen B-S & Hampsey M (2004) Functional interaction between TFIIB and the Rpb2 subunit of RNA polymerase II: implications for the mechanism of transcription initiation. *Mol Cell Biol* **24**: 3983–91
- Cheung ACM, Sainsbury S & Cramer P (2011) Structural basis of initial RNA polymerase II transcription. *EMBO J.* **30**: 4755–63
- Duchi D, Bauer DLV, Fernandez L, Evans G, Robb N, Hwang LC, Gryte K, Tomescu A, Zawadzki P, Morichaud Z, Brodolin K & Kapanidis AN (2016) RNA Polymerase Pausing during Initial Transcription. *Mol. Cell* **63**: 939–950
- Dulin D, Bauer DLV, Malinen AM, Bakermans JJW, Kaller M, Morichaud Z, Petushkov I, Depken M, Brodolin K, Kulbachinskiy A & Kapanidis AN (2018) Pausing controls branching between productive and non-productive pathways during initial transcription in bacteria. *Nat. Commun.* **9**: Available at: <http://www.nature.com/articles/s41467-018-03902-9>
- Durniak KJ, Bailey S & Steitz TA (2008) The structure of a transcribing T7 RNA polymerase in transition from initiation to elongation. *Science* **322**: 553–7
- Emsley P & Cowtan K (2004) Coot: model-building tools for molecular graphics. *Acta Crystallogr. D Biol. Crystallogr.* **60**: 2126–2132
- Geszvain K, Gruber TM, Mooney RA, Gross CA & Landick R (2004) A hydrophobic patch on the flap-tip helix of E.coli RNA polymerase mediates sigma(70) region 4 function. *J Mol Biol* **343**: 569–87
- Hein PP, Palangat M, Landick R. (2011) RNA transcript 3'-proximal sequence affects translocation bias of RNA polymerase. *Biochemistry.* **50**:7002-14.
- Hein PP, Kolb KE, Windgassen T, Bellecourt MJ, Darst SA, Mooney RA & Landick R (2014) RNA polymerase pausing and nascent-RNA structure formation are linked through clamp-domain movement. *Nat. Publ. Group* **21**: 794–802
- Hinton DM & Vuthoori S (2000) Efficient inhibition of Escherichia coli RNA polymerase by the

bacteriophage T4 AsiA protein requires that AsiA binds first to free sigma70. *J. Mol. Biol.* **304**: 731–739

Hu Y, Morichaud Z, Perumal AS, Roquet-Baneres F & Brodolin K (2014) Mycobacterium RbpA cooperates with the stress-response σ B subunit of RNA polymerase in promoter DNA unwinding. *Nucleic Acids Res* **42**: 10399–408

Huang Y, Chen C & Russu IM (2009) Dynamics and stability of individual base pairs in two homologous RNA-DNA hybrids. *Biochemistry* **48**: 3988–3997

Kang JY, Mishanina TV, Bellecourt MJ, Mooney RA, Darst SA & Landick R (2018) RNA Polymerase Accommodates a Pause RNA Hairpin by Global Conformational Rearrangements that Prolong Pausing. *Mol. Cell* **69**: 802–815.e5

Kapanidis AN, Margeat E, Ho SO, Kortkhonjia E, Weiss S & Ebright RH (2006) Initial transcription by RNA polymerase proceeds through a DNA-scrunching mechanism. *Science* **314**: 1144–1147

Kireeva ML, Komissarova N, Waugh DS & Kashlev M (2000) The 8-nucleotide-long RNA:DNA hybrid is a primary stability determinant of the RNA polymerase II elongation complex. *J Biol Chem* **275**: 6530–6

Kostrewa D, Zeller ME, Armache K-J, Seizl M, Leike K, Thomm M & Cramer P (2009) RNA polymerase II-TFIIB structure and mechanism of transcription initiation. *Nature* **462**: 323–330

Kubori T & Shimamoto N (1996) A Branched Pathway in the Early Stage of Transcription by Escherichia coli RNA Polymerase. *J. Mol. Biol.* **256**: 449–457

Kulbachinskiy A & Mustaev A (2006) Region 3.2 of the sigma subunit contributes to the binding of the 3'-initiating nucleotide in the RNA polymerase active center and facilitates promoter clearance during initiation. *J Biol Chem* **281**: 18273–6

Kulbachinskiy AV, Ershova GV, Korzheva NV, Brodolin KL & Nikiforov VG (2002) Mutations in β '-Subunit of the Escherichia coli RNA-Polymerase Influence Interaction with the Downstream DNA Duplex in the Elongation Complex. *Russ. J. Genet.* **38**: 1207–1211

Kumar A, Grimes B, Fujita N, Makino K, Malloch RA, Hayward RS & Ishihama A (1994) Role of

the sigma 70 subunit of Escherichia coli RNA polymerase in transcription activation. *J Mol Biol* **235**: 405–13

- Kumar A, Malloch RA, Fujita N, Smillie DA, Ishihama A & Hayward RS (1993) The minus 35-recognition region of Escherichia coli sigma 70 is inessential for initiation of transcription at an ‘extended minus 10’ promoter. *J Mol Biol* **232**: 406–18
- Kuznedelov K, Minakhin L, Niedziela-Majka A, Dove SL, Rogulja D, Nickels BE, Hochschild A, Heyduk T & Severinov K (2002) A role for interaction of the RNA polymerase flap domain with the sigma subunit in promoter recognition. *Science* **295**: 855–7
- Lane WJ & Darst SA (2010) Molecular Evolution of Multisubunit RNA Polymerases: Sequence Analysis. *J. Mol. Biol.* **395**: 671–685
- Li L, Molodtsov V, Lin W, Ebright RH & Zhang Y (2020) RNA extension drives a stepwise displacement of an initiation-factor structural module in initial transcription. *Proc. Natl. Acad. Sci. U. S. A.* **117**: 5801–5809
- Lin W, Mandal S, Degen D, Liu Y, Ebright YW, Li S, Feng Y, Zhang Y, Mandal S, Jiang Y, Liu S, Gigliotti M, Talaue M, Connell N, Das K, Arnold E & Ebright RH (2017) Structural Basis of Mycobacterium tuberculosis Transcription and Transcription Inhibition. *Mol. Cell* **66**: 169–179.e8
- Liu X, Bushnell D a, Silva D-A, Huang X & Kornberg RD (2011) Initiation complex structure and promoter proofreading. *Science* **333**: 633–637
- Liu X, Bushnell DA, Wang D, Calero G & Kornberg RD (2010) Structure of an RNA polymerase II-TFIIB complex and the transcription initiation mechanism. *Science* **327**: 206–9
- Metzger W, Schickor P, Meier T, Werel W & Heumann H (1993) Nucleation of RNA Chain Formation by Escherichia coli DNA-dependent RNA Polymerase. *J. Mol. Biol.* **232**: 35–49
- Morichaud Z, Chaloin L & Brodolin K (2016) Regions 1.2 and 3.2 of the RNA Polymerase σ Subunit Promote DNA Melting and Attenuate Action of the Antibiotic Lipiarmycin. *J. Mol. Biol.* **428**: 463–76
- Murakami KS, Masuda S & Darst S a (2002) Structural basis of transcription initiation: RNA polymerase holoenzyme at 4 Å resolution. *Science* **296**: 1280–1284

- Nudler E, Mustaev A, Lukhtanov E & Goldfarb A (1997) The RNA-DNA hybrid maintains the register of transcription by preventing backtracking of RNA polymerase. *Cell* **89**: 33–41
- Pettersen EF, Goddard TD, Huang CC, Couch GS, Greenblatt DM, Meng EC & Ferrin TE (2004) UCSF Chimera—a visualization system for exploratory research and analysis. *J Comput Chem* **25**: 1605–12
- Pupov D, Kuzin I, Bass I & Kulbachinskiy A (2014) Distinct functions of the RNA polymerase σ subunit region 3.2 in RNA priming and promoter escape. *Nucleic Acids Res.* **42**: 4494–4504
- Ruff EF, Record MT & Artsimovitch I (2015) Initial events in bacterial transcription initiation. *Biomolecules* **5**: 1035–1062
- Saecker RM, Record MTJ & Dehaseth PL (2011) Mechanism of bacterial transcription initiation: RNA polymerase - promoter binding, isomerization to initiation-competent open complexes, and initiation of RNA synthesis. *J Mol Biol* **412**: 754–71
- Sainsbury S, Niesser J & Cramer P (2013) Structure and function of the initially transcribing RNA polymerase II-TFIIB complex. *Nature* **493**: 437–40
- Shi J, Wen A, Zhao M, You L, Zhang Y & Feng Y (2019) Structural basis of σ appropriation. *Nucleic Acids Res.* **47**: 9423–9432
- Sidorenkov I, Komissarova N & Kashlev M (1998) Crucial role of the RNA:DNA hybrid in the processivity of transcription. *Mol Cell* **2**: 55–64
- Touloukhonov I, Artsimovitch I & Landick R (2001) Allosteric Control of RNA Polymerase by a Site That Contacts Nascent RNA Hairpins. *Science* **292**: 730–733
- Touloukhonov I & Landick R (2003) The flap domain is required for pause RNA hairpin inhibition of catalysis by RNA polymerase and can modulate intrinsic termination. *Mol. Cell* **12**: 1125–1136
- Touloukhonov I, Zhang J, Palangat M & Landick R (2007a) A Central Role of the RNA Polymerase Trigger Loop in Active-Site Rearrangement during Transcriptional Pausing. *Mol. Cell* **27**: 406–419
- Touloukhonov I, Zhang J, Palangat M & Landick R (2007b) A central role of the RNA polymerase

trigger loop in active-site rearrangement during transcriptional pausing. *Mol Cell* **27**: 406–19

Tupin A, Gualtieri M, Leonetti J-P & Brodolin K (2010) The transcription inhibitor lipiarmycin blocks DNA fitting into the RNA polymerase catalytic site. *EMBO J* **29**: 2527–37

Vassilyev DG, Vassilyeva MN, Perederina A, Tahirov TH & Artsimovitch I (2007a) Structural basis for transcription elongation by bacterial RNA polymerase. *Nature* **448**: 157–162

Vassilyev DG, Vassilyeva MN, Zhang J, Palangat M, Artsimovitch I & Landick R (2007b) Structural basis for substrate loading in bacterial RNA polymerase. *Nature* **448**: 163–168

Vishwakarma RK, Cao A-M, Morichaud Z, Perumal AS, Margeat E & Brodolin K (2018) Single-molecule analysis reveals the mechanism of transcription activation in *M. tuberculosis*. *Sci. Adv.* **4**: eaao5498

Vvedenskaya IO, Vahedian-Movahed H, Bird JG, Knoblauch JG, Goldman SR, Zhang Y, Ebright RH & Nickels BE (2014) Transcription. Interactions between RNA polymerase and the ‘core recognition element’ counteract pausing. *Science* **344**: 1285–9

Weixlbaumer A, Leon K, Landick R & Darst S a. (2013) Structural basis of transcriptional pausing in bacteria. *Cell* **152**: 431–441

Werner F & Weinzierl ROJ (2005) Direct Modulation of RNA Polymerase Core Functions by Basal Transcription Factors. *Mol. Cell. Biol.* **25**: 8344–8355

Zenkin N, Kulbachinskiy A, Yuzenkova Y, Mustaev A, Bass I, Severinov K & Brodolin K (2007) Region 1.2 of the RNA polymerase sigma subunit controls recognition of the -10 promoter element. *EMBO J.* **26**: 955–964

Zenkin N, Naryshkina T, Kuznedelov K & Severinov K (2006) The mechanism of DNA replication primer synthesis by RNA polymerase. *Nature* **439**: 617–620

Zenkin N & Severinov K (2004) The role of RNA polymerase sigma subunit in promoter-independent initiation of transcription. *Proc. Natl. Acad. Sci. U. S. A.* **101**: 4396–4400

Zhang J, Palangat M & Landick R (2010) Role of the RNA polymerase trigger loop in catalysis and pausing. *Nat Struct Mol Biol* **17**: 99–104

Zhang Y, Feng Y, Chatterjee S, Tuske S, Ho MX, Arnold E & Ebright RH (2012) Structural basis of transcription initiation. *Science* **338**: 1076–80

FIGURE LEGENDS

Figure 1. The σ subunit stimulates *de novo* transcription initiation on promoter-less DNA scaffolds.

(A). Scheme of the synthetic DNA scaffolds: Short Duplex Template (SDT) and Long Duplex Template (LDT). Blue, template strand; red, non-template DNA strand. The position of the σ 3.2-finger (σ 3.2) is indicated by a gray rectangle. (B). Transcription initiation by wild type (WT) *Eco*RNAP, or harboring the indicated mutant σ^{70} variants, at the SDT and LDT scaffolds in the presence of CTP, GTP and [α - 32 P]-UTP. The bar graph shows the RNA product quantification. The RNA amount in each lane was normalized to the RNA synthesized in the presence of the full length σ^{70} subunit. (C). Inhibition of transcription on SDT by 10 μ M rifampicin (Rif). (D). Scheme showing the σ^{70} subunit with domains 1 to 4. NCR, non-conserved region. The regions interacting with the promoter -10 and -35 consensus elements are indicated. The organization of the mutant σ^{70} variants is shown with black lines underneath the scheme. The σ 3.2-finger sequence (amino acids 513-519) deleted in the $\sigma_{\Delta 3.2}$ mutant is shown in purple letters. (E). Structural models of the *Eco*RNAP core (left) and holoenzyme (right) (PDB: 6C9Y) shown as semitransparent surfaces in complex with scaffold DNA (blue-red) (DNA and RNA from PDB: **2O5I**). The core is in complex with 14-nt RNA (yellow-orange-purple) and the holoenzyme is in complex with 4-nt RNA (yellow-orange). The RNA 5'-phosphates are shown as spheres. The 5' end nucleotide is colored in orange. The σ^{70} subunit is shown as ribbons with the conserved regions colored as in **panel D**. The C α atoms of amino acids 513-519 in region 3.2 are shown as spheres. (F). Transcriptional activity of the *Eco*RNAP holoenzyme harboring mutant σ^{70} variants. Transcription was initiated at the *lacUV5* promoter by the ApA primer and [α - 32 P]-UTP and at the *galP1*cons promoter by the CpA primer, [α - 32 P]-UTP and ATP. The RNA product sequences are indicated.

Figure 2. The σ subunit and DNA template architecture modulate forward translocation.

(A). Scheme of the primer extension reaction on the LDT scaffold. The RNA primers (pRNA) used to assemble Initial Transcribing Complexes (ITCs) are shown in red. Nucleotides added during initial transcription are in purple. The position of the σ 3.2-finger is indicated by a gray rectangle. (B). Simplified scheme of the nucleotide addition cycle (NAC) on scaffold DNA template (blue) with a 2-nt RNA primer (red) and initiating 3' UTP (purple). The active site registers are designated as i and i+1. TL, trigger loop; TH, trigger helix. (C). Extension of 2-nt pRNA (pRNA2) by *Eco*RNAP on the LDT scaffold in the presence of wild type (WT) or mutant σ^{70} variants. The stacked bar graph shows the RNA product quantification. The RNA amount in each lane was normalized to the total RNA synthesized in the presence of the full length σ^{70} subunit. (D). Scheme of the SDT2 and SDT2+1 scaffolds with 6-nt nascent RNA. Red, sequence of the 3-nt

544 pRNA; purple, nucleotides added during primer extension. (E). Transcription initiation by *Eco*RNAP at the
545 SDT2 and SDT2+1 scaffolds with 3-nt pRNA (pRNA3) in the presence of mutant σ^{70} variants. The stacked
546 bar graph shows the RNA product quantification. The amounts of 4-nt and 6-nt RNA in each lane were
547 normalized to the total RNA (4-nt + 6-nt) amount in each lane.

548

549 **Figure 3. The σ subunit regions 3.2 and 4 stabilize short RNAs in ITCs.**

550 (A). Scheme of the LDT scaffold with the RNA primers (pRNA) used to assemble ITC2 - ITC6. (B, C, D).
551 [α - 32 P]-UTP-labeled RNAs produced in primer extension reactions in the presence of σ^{70} , $\sigma\Delta 3.2$, and $\sigma\Delta 4$,
552 respectively. ITCs were immobilized on Ni $^{2+}$ -agarose beads and washed (Ni-bound) or not (Total) with buffer
553 (TB), as indicated, before labeling. The experimental setup is shown schematically on top of panel B. (E).
554 Quantification of the results shown in panels B,C,D. The fraction of labeled RNA retained in ITCn was
555 calculated as the ratio between the RNA amount in the washed ITCn (Ni-bound) to the RNA amount in the
556 unwashed ITCn (Total). (F). Comparison of the retention efficiency for 4-nt RNA in the presence of σ^{70}
557 (WT), $\sigma\Delta 3.2$ and $\sigma\Delta 4.2$. The number of washing steps is indicated; w/o, without washes. (G). Quantification
558 of the results shown in panel F. The fraction of labeled RNA retained in ITC4 is plotted as a function of the
559 washing step number. The RNA amount in each lane was normalized to the RNA in unwashed ITC4.

560

561 **Figure 4. RNA:DNA hybrid and σ modulate RNAP translocation efficiency.**

562 (A). Scheme of the SDT scaffold with primer RNAs (pRNA) of various lengths (red) used to assemble ITC2
563 - ITC7. Nucleotides added during initial transcription are in purple. (B). Primer extension reactions, shown
564 schematically at the top, were performed with the pRNAs shown in panel A in the presence or absence of the
565 indicated σ^{70} variants. (C). Quantification of the experiments shown in panel B. The values of RNA[n+3] for
566 each lane were normalized to the total RNA (RNA[n+1] + RNA[n+3]) in each lane and were plotted as a
567 function of the RNA length. (D, E). Structural models of the σ^{70} subunit-DNA-RNA interactions in the
568 RNAP main channel. The $\sigma 3.2$ finger (PDB: **4YG2**) is shown as a molecular surface. The coordinates of the
569 DNA template strand (in blue) and RNA are from PDB: **2O5I**. RNA 5'-phosphates are shown as spheres
570 colored in function of the RNA length. The RNA 3' end is in yellow, the RNA 5' end nucleotides that clash
571 with $\sigma 3.2$ -finger are in magenta. The nucleotide in the fourth position, marking the transition from unstable
572 to stable ITC, is in orange. (E). The same as in panel D, with the $\sigma 3.2$ -finger residues (aa 513-519) deleted.
573 Models were built with COOT (Emsley & Cowtan, 2004) and UCSF Chimera (Pettersen *et al*, 2004).

574

575 **Figure 5. The RNA 3' end nucleotide modulates the initial pause duration.**

576 (A). Scheme of SDT2 and SDT-G scaffolds with 3-nt primer RNA (pRNA3). The primer extension reactions
577 were performed with [α - 32 P]-UTP on the SDT scaffold and with [α - 32 P]-CTP on the SDT-G scaffold. (B).
578 Kinetics of primer extension at the SDT scaffold. (C). Quantification of the experiment shown in panel B.
579 The left graph shows the synthesis of total RNA over time. The right graph shows the RNA product

fractions, representing the different ITCs, over time. For each time point, values were normalized to the total RNA synthesized at that time point. **(D)**. Pause half-life times ($t_{1/2}$) calculated from the experiments shown in panels B and E. **(E)**. Kinetics of primer extension on the SDT-G scaffold. **(F)**. Quantification of the experiment shown in panel E.

Figure 6. The σ -remodeling factors AsiA and RbpA modulate initial transcription.

(A). Structural model of the σ^{70} -*Eco*RNAP holoenzyme (PDB: **4YG2**) in complex with the SDT scaffold DNA and 3-nt RNA (yellow). Core RNA is shown as molecular surfaces. The β subunit is shown as a transparent surface. The σ subunit is shown as a ribbon in which the $\sigma 4$ domain is in dark red, the σ region 3.2 is in cyan, and the other regions are in gray. The β -Flap (G891-G907) is shown as a ribbon (cornflower blue). The remodeled conformation of the $\sigma 4$ domain ($\sigma 4$ -AsiA) in the *Eco*RNAP-AsiA-MotA complex (PDB: **6K4Y**) is shown in light green. The C α atoms of the σ^{70} residues 528 and 553, shown as spheres, mark the borders of the $\sigma \Delta 4$ and $\sigma \Delta 4.2$ deletions, respectively. **(B)**. Transcription initiation at the *lacUV5* promoter and SDT2 scaffold in the presence or not of AsiA. Transcription was initiated by ApA and [α - 32 P]-UTP (lanes 1,2), by the GpC primer, GTP and [α - 32 P]-UTP (lanes 3-6), or by CTP, GTP and [α - 32 P]-UTP (lanes 7,8). **(C)**. Quantification of the experiments shown in panel B. For each experimental condition (-/+ AsiA), the amount of each RNA product was normalized to the total RNA synthesized without AsiA. Averages and standard errors of two independent experiments are shown. **(D)** Structural model of σ^A -*Mtb*RNAP (PDB: **6EDT**) in complex with RbpA (green ribbon) and the SDT scaffold DNA. The nomenclature and color code are the same as in panel A. **(E)** Primer extension reactions performed by the *Mtb*RNAP core and σ^B -*Mtb*RNAP holoenzyme on the SDT2 scaffold with and without RbpA. Transcription was initiated by GTP and [α - 32 P]-UTP. **(F)** Primer extension reactions performed by the *Mtb*RNAP^{AFTH} core and σ^B -*Mtb*RNAP^{AFTH} holoenzyme on the SDT2 scaffold with and without RbpA. Transcription was initiated by GTP and [α - 32 P]-UTP. **(G)**. Quantification of the results shown in panels E and F, performed as in Figure 4C.

Figure 7. Model of events during initial transcription.

(A). Schematic representation of RNAP in complex with DNA template. Bases corresponding to the scaffold DNA template are in blue. The RNA primer is in red. The σ subunit domains are shown as rectangles in blue ($\sigma 2$ -3) and green ($\sigma 4$). The active site registers are indicated as “i” and “i+1”. **(B)**. Scheme of events during transition from ITC to elongation complex (EC). The upper images shows productive ITCs and paused ITCs (PITC) in complex with the LDT scaffold. Bases corresponding to the SDT scaffold are shown in blue. ITCs are shown in the pre-translocated (ITC^{Pre}) and post-translocated (ITC^{Post}) states. The gray gradients in the lower part of the panel indicate the probability level of abortive transcription and initial pausing, and the accomplishment levels of RNA:DNA hybrid formation, σ displacement and ejection.

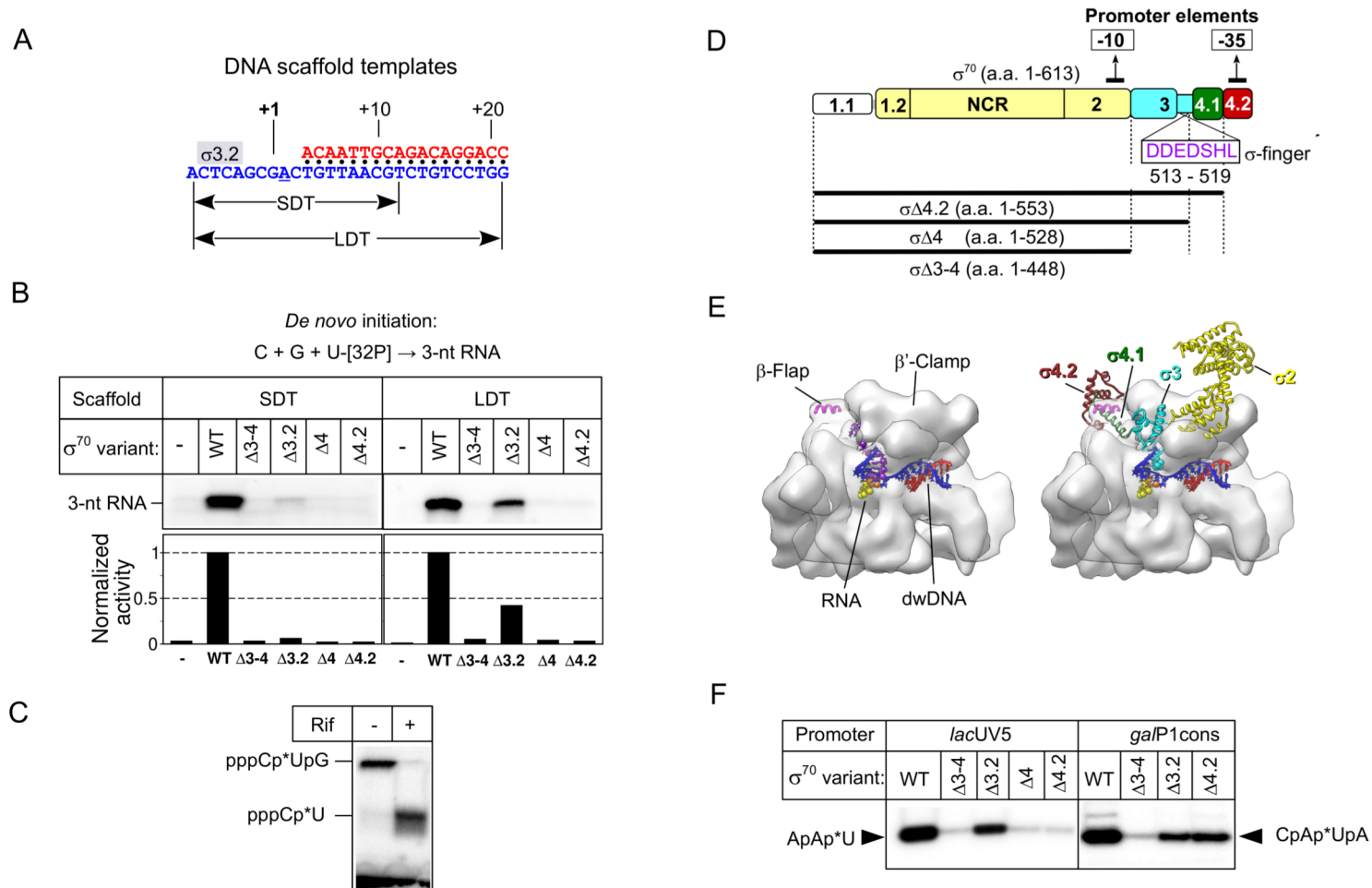
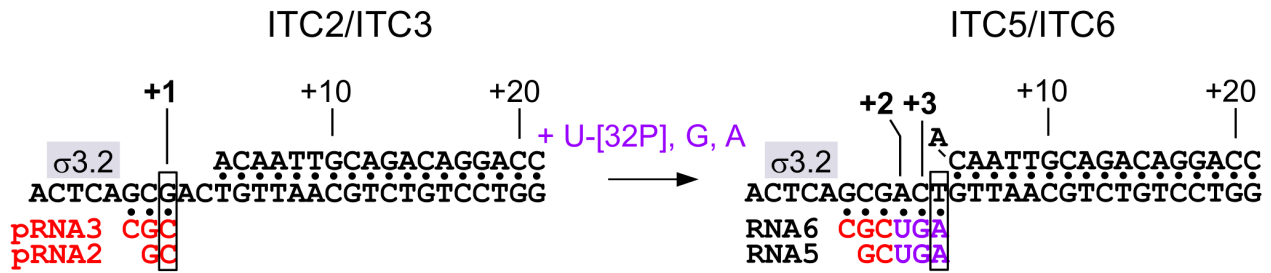
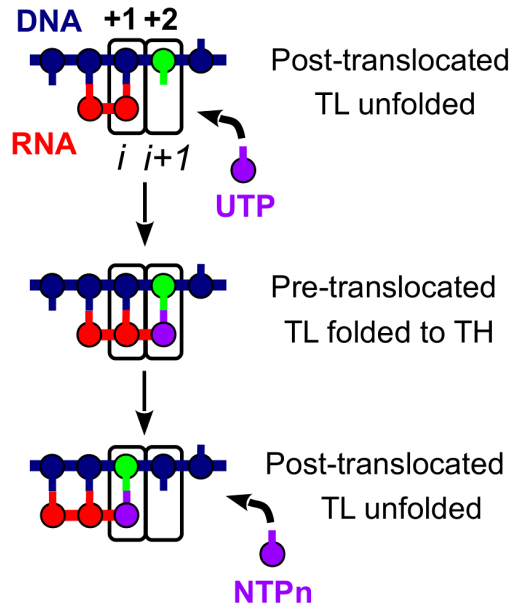


Figure 1

A



B

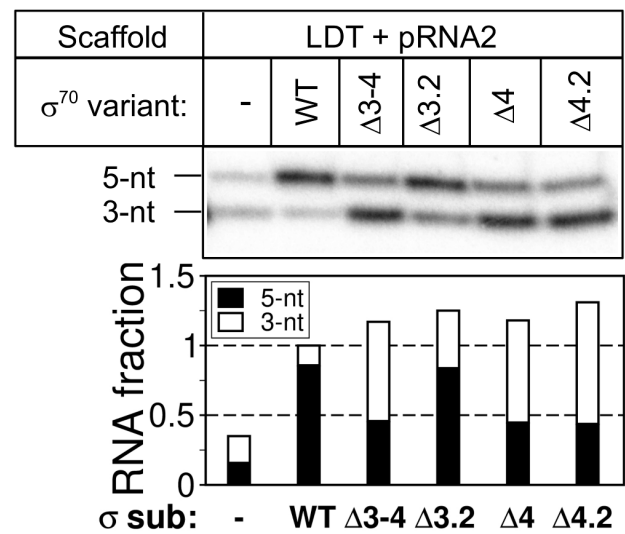


C

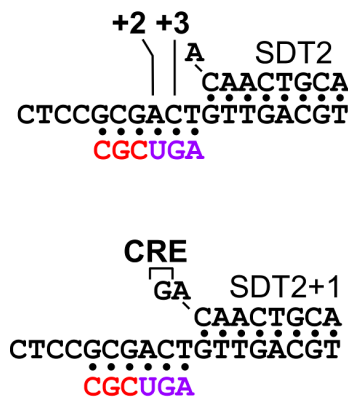
Primer extension reaction:

(1) GpC + U-[32P] → GpCpU* (3-nt RNA)

(2) GpCpU* + G + A → GpCpU*pGpA (5-nt RNA)



D



E

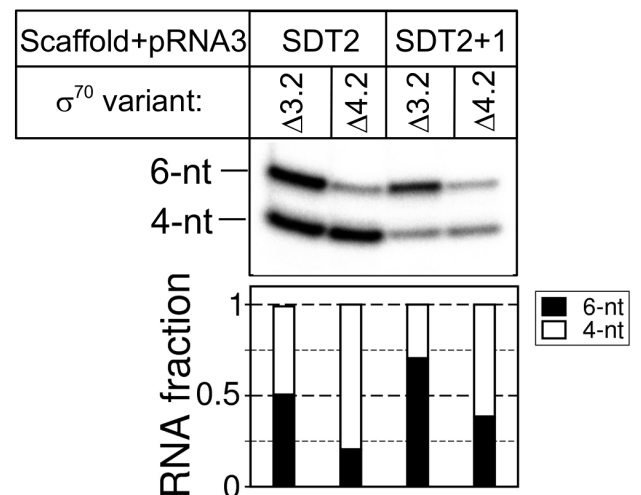


Figure 2

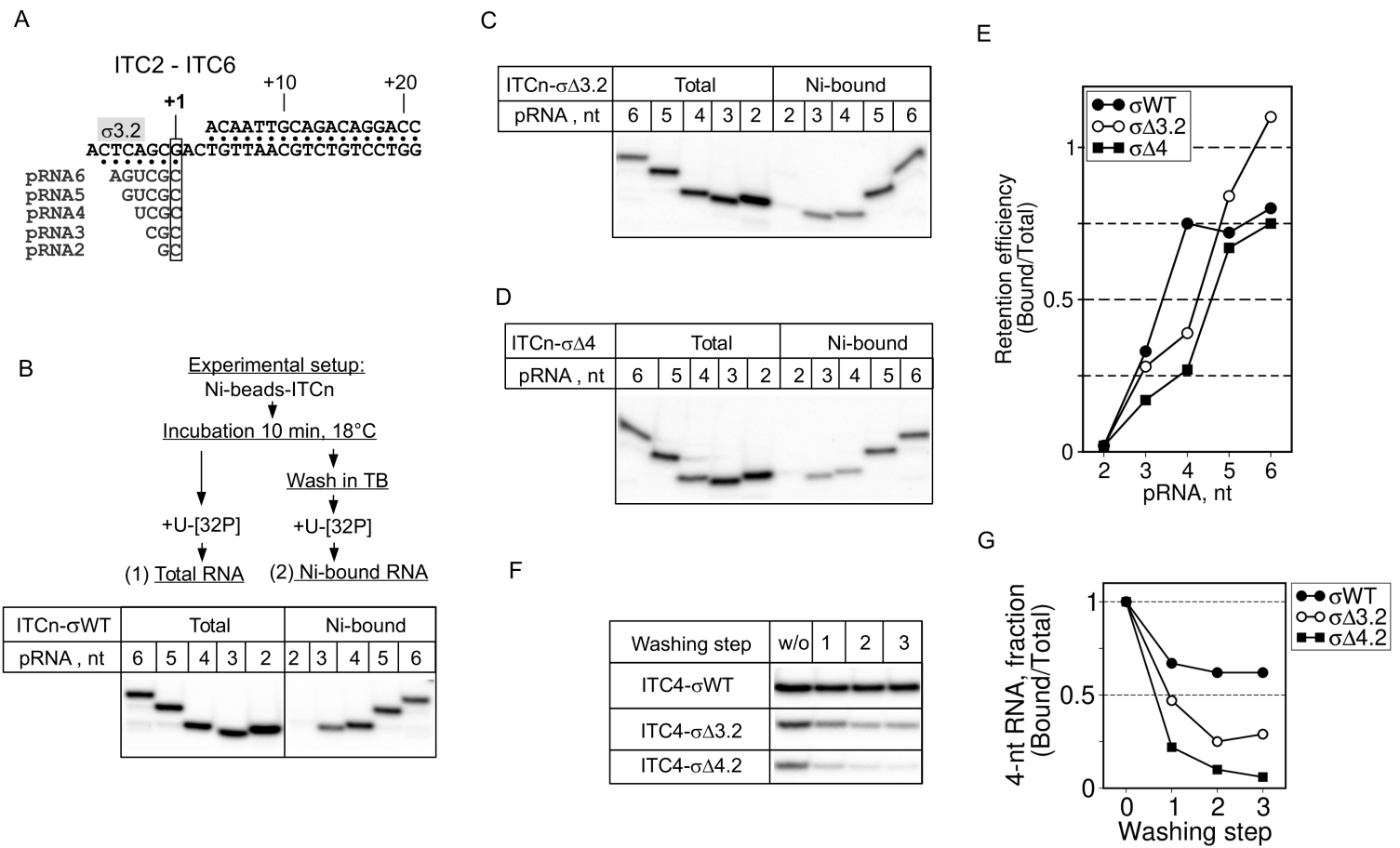


Figure 3

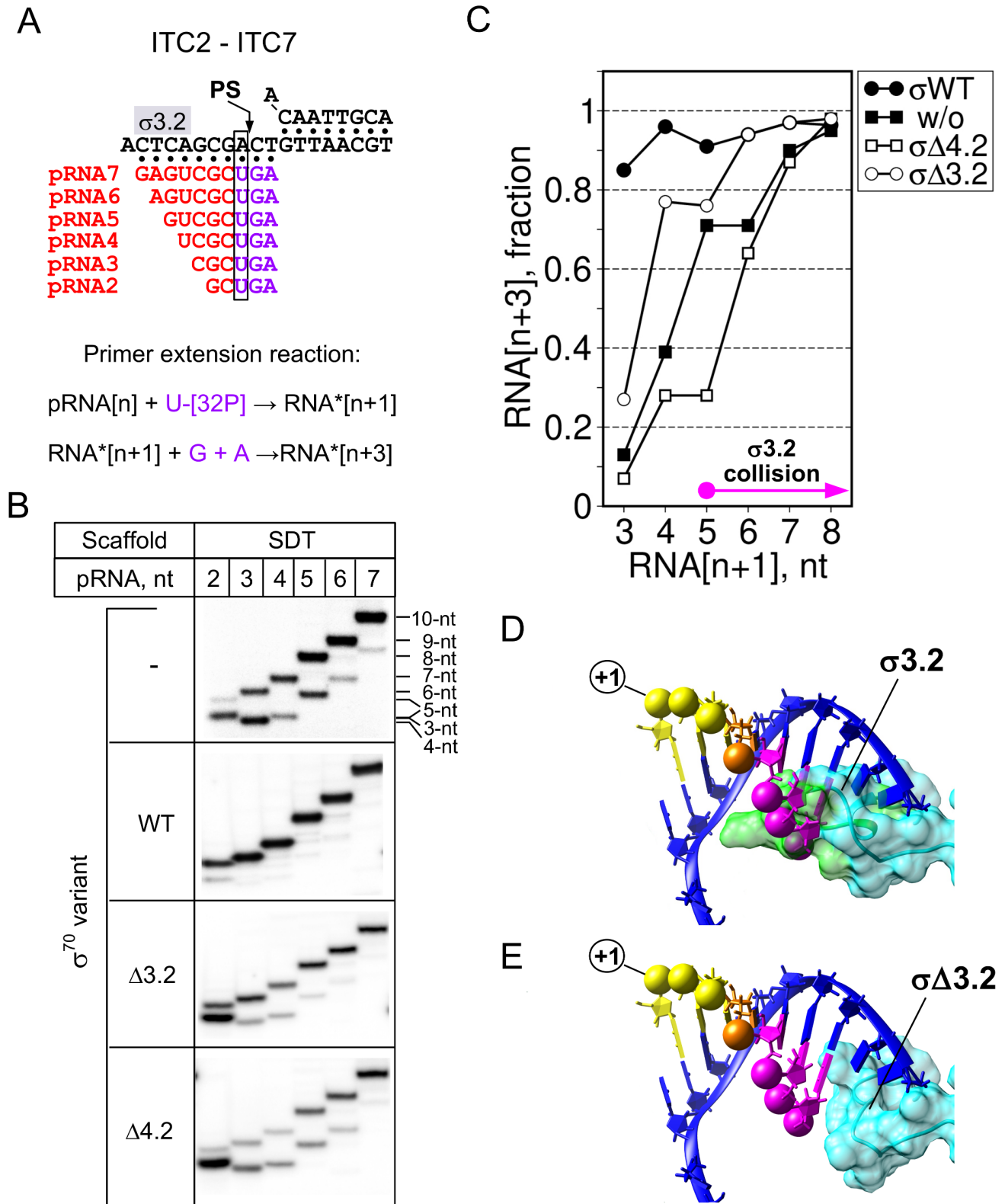
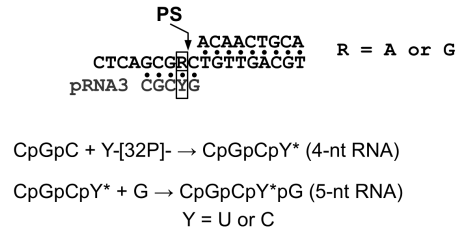
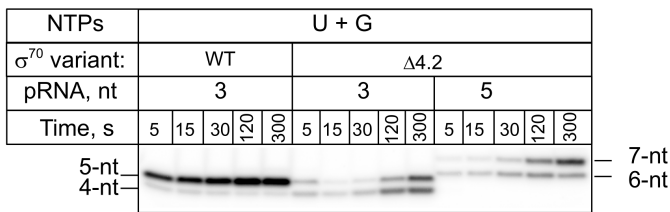


Figure 4

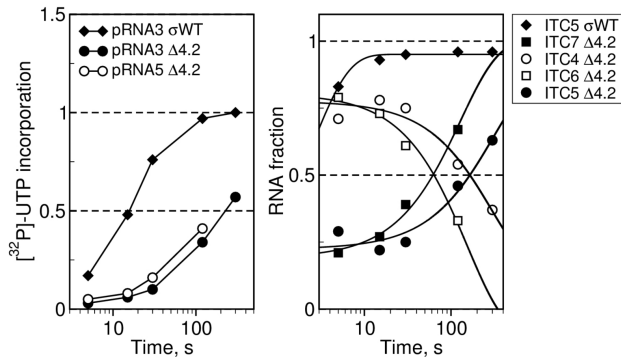
A



B



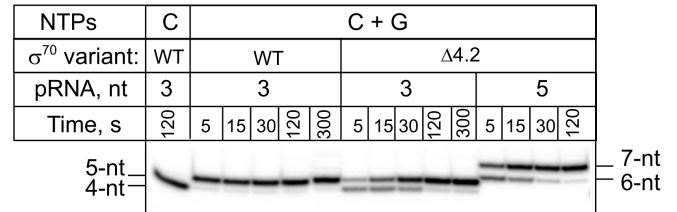
C



D

σ^{70} variant	ITC4 pause $t_{1/2}$ (s)		ITC6 pause $t_{1/2}$ (s)	
	3'- U	3'- C	3'- U	3'- C
WT	1,69	< 1,03	ND	ND
$\Delta 4.2$	204	16,5	86	8,6

E



F

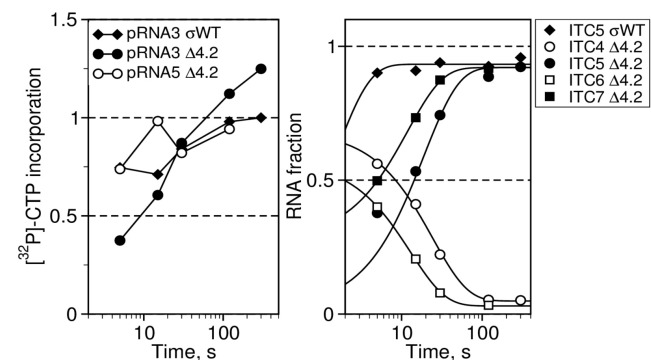


Figure 5

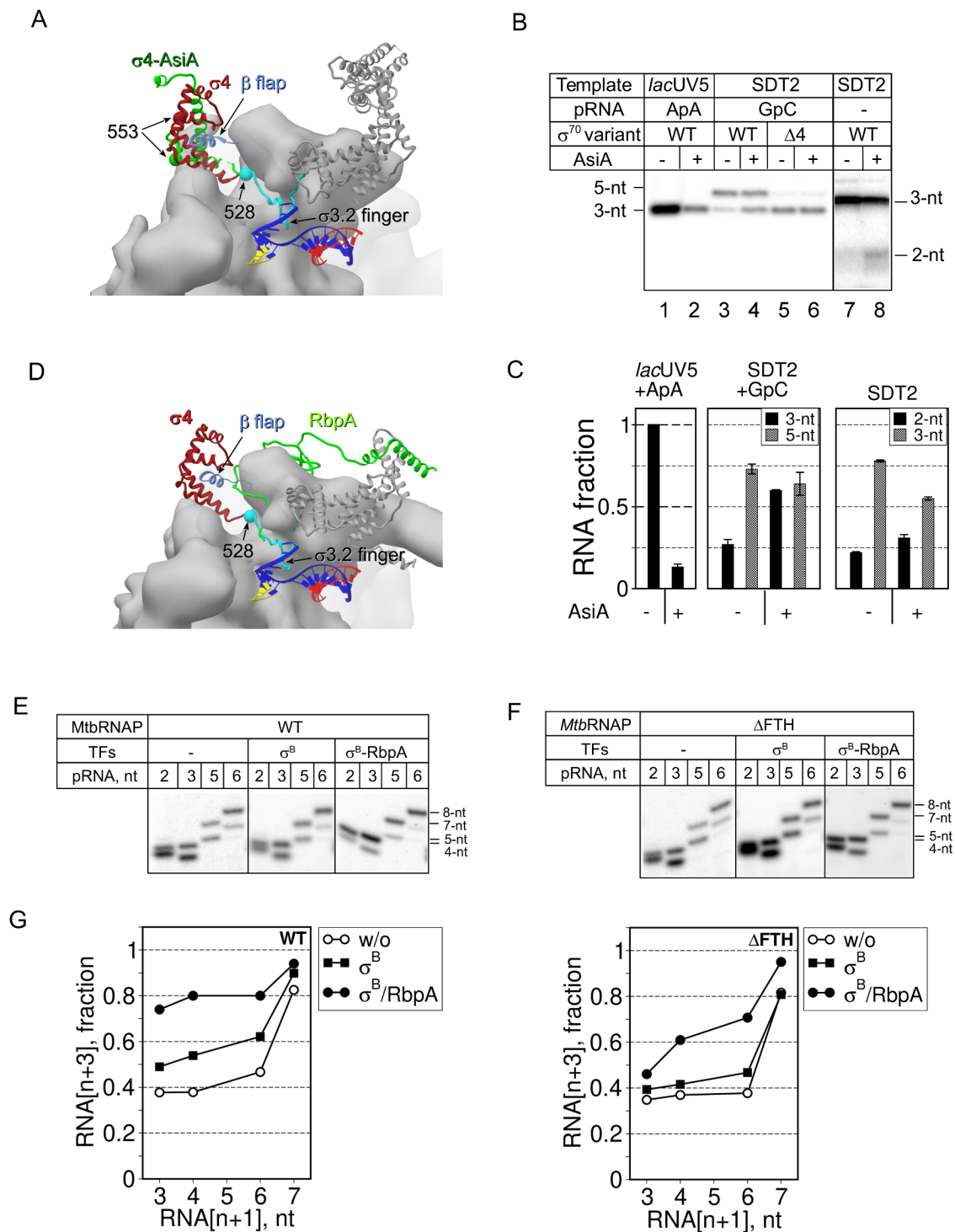


Figure 6

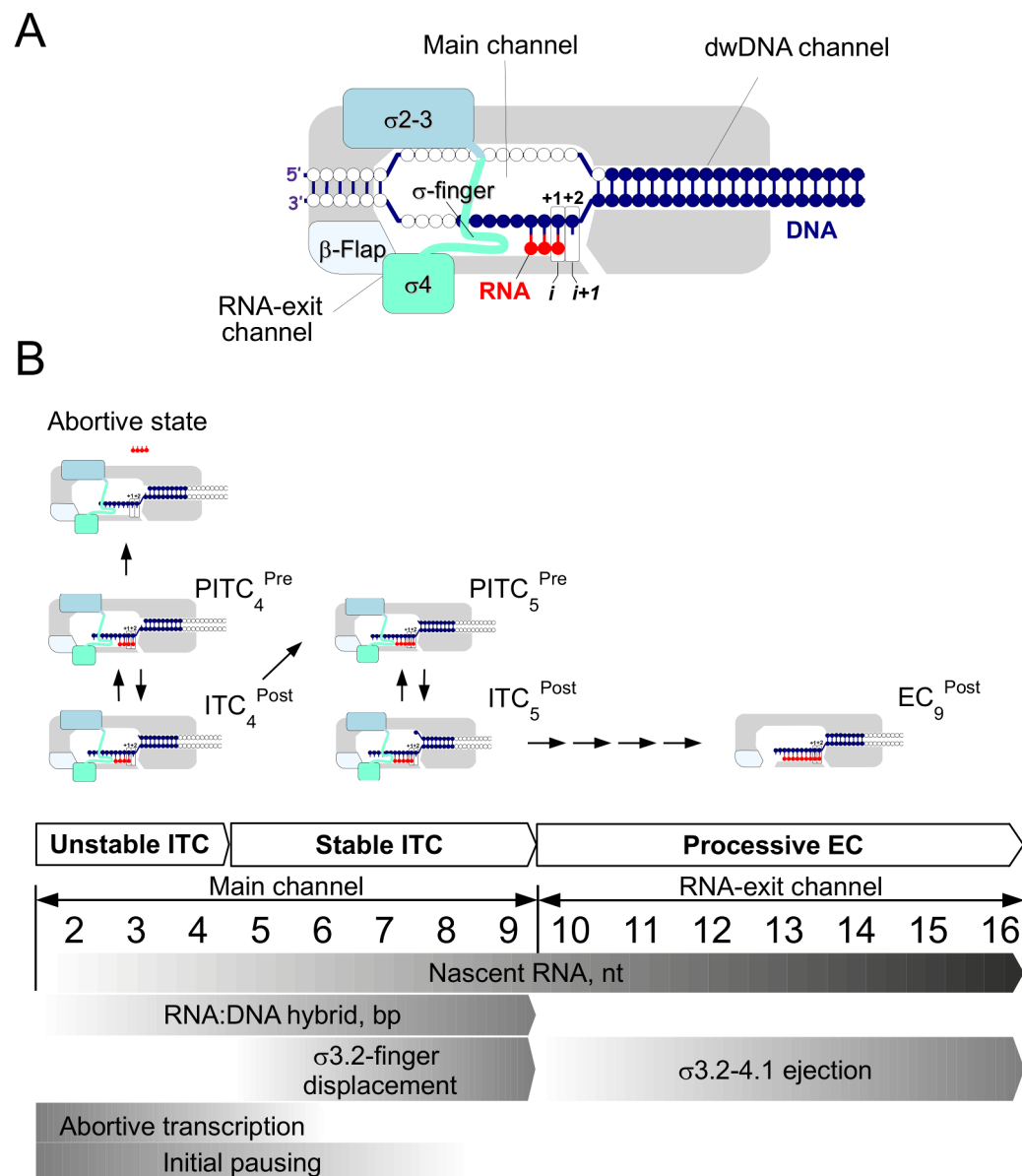


Figure 7